

## Visual seizure annotation and automated seizure detection using behind-the-ear electroencephalographic channels

Vandecasteele, Kaat; De Cooman, Thomas; Dan, Jonathan; Cleeren, Evy; Van Huffel, Sabine; Hunyadi, Borbála; Van Paesschen, Wim

**DOI**

[10.1111/epi.16470](https://doi.org/10.1111/epi.16470)

**Publication date**

2020

**Document Version**

Final published version

**Published in**

Epilepsia

**Citation (APA)**

Vandecasteele, K., De Cooman, T., Dan, J., Cleeren, E., Van Huffel, S., Hunyadi, B., & Van Paesschen, W. (2020). Visual seizure annotation and automated seizure detection using behind-the-ear electroencephalographic channels. *Epilepsia*, 61(4), 766-775. <https://doi.org/10.1111/epi.16470>

**Important note**

To cite this publication, please use the final published version (if applicable). Please check the document version above.

**Copyright**

Other than for strictly personal use, it is not permitted to download, forward or distribute the text or part of it, without the consent of the author(s) and/or copyright holder(s), unless the work is under an open content license such as Creative Commons.

**Takedown policy**

Please contact us and provide details if you believe this document breaches copyrights. We will remove access to the work immediately and investigate your claim.



# Visual seizure annotation and automated seizure detection using behind-the-ear electroencephalographic channels

Kaat Vandecasteele<sup>1</sup> | Thomas De Cooman<sup>1</sup> | Jonathan Dan<sup>1,2</sup> | Evy Cleeren<sup>3</sup> | Sabine Van Huffel<sup>1</sup> | Borbála Hunyadi<sup>4</sup> | Wim Van Paesschen<sup>3,5</sup>

<sup>1</sup>Department of Electrical Engineering (ESAT), STADIUS Center for Dynamical Systems, Signal Processing and Data Analytics, KU Leuven, Leuven, Belgium

<sup>2</sup>Byteflies, Antwerp, Belgium

<sup>3</sup>Department of Neurology, UZ Leuven, Leuven, Belgium

<sup>4</sup>Department of Microelectronics, Delft University of Technology, Delft, the Netherlands

<sup>5</sup>Laboratory for Epilepsy Research, KU Leuven, Leuven, Belgium

## Correspondence

Kaat Vandecasteele, Department of Electrical Engineering (ESAT), STADIUS Center for Dynamical Systems, Signal Processing and Data Analytics, KU Leuven, Kasteelpark Arenberg 10 - Bus 2446, 3001 Leuven, Belgium.

Email: kaat.vandecasteele@esat.kuleuven.be

## Funding information

EIT, Grant/Award Number: 19263 SeizeIT2

## Abstract

**Objective:** Seizure diaries kept by patients are unreliable. Automated electroencephalography (EEG)-based seizure detection systems are a useful support tool to objectively detect and register seizures during long-term video-EEG recording. However, this standard full scalp-EEG recording setup is of limited use outside the hospital, and a discreet, wearable device is needed for capturing seizures in the home setting. We are developing a wearable device that records EEG with behind-the-ear electrodes. In this study, we determined whether the recognition of ictal patterns using only behind-the-ear EEG channels is possible. Second, an automated seizure detection algorithm was developed using only those behind-the-ear EEG channels.

**Methods:** Fifty-four patients with a total of 182 seizures, mostly temporal lobe epilepsy (TLE), and 5284 hours of data, were recorded with a standard video-EEG at University Hospital Leuven. In addition, extra behind-the-ear EEG channels were recorded. First, a neurologist was asked to annotate behind-the-ear EEG segments containing selected seizure and nonseizure fragments. Second, a data-driven algorithm was developed using only behind-the-ear EEG. This algorithm was trained using data from other patients (patient-independent model) or from the same patient (patient-specific model).

**Results:** The visual recognition study resulted in 65.7% sensitivity and 94.4% specificity. By using those seizure annotations, the automated algorithm obtained 64.1% sensitivity and 2.8 false-positive detections (FPs)/24 hours with the patient-independent model. The patient-specific model achieved 69.1% sensitivity and 0.49 FPs/24 hours.

**Significance:** Visual recognition of ictal EEG patterns using only behind-the-ear EEG is possible in a significant number of patients with TLE. A patient-specific seizure detection algorithm using only behind-the-ear EEG was able to detect more seizures automatically than what patients typically report, with 0.49 FPs/24 hours.

Borbála Hunyadi and Wim Van Paesschen share last authorship.

This is an open access article under the terms of the Creative Commons Attribution-NonCommercial License, which permits use, distribution and reproduction in any medium, provided the original work is properly cited and is not used for commercial purposes.

© 2020 The Authors. *Epilepsia* published by Wiley Periodicals, Inc. on behalf of International League Against Epilepsy

We conclude that a large number of refractory TLE patients can benefit from using this device.

**KEYWORDS**

automated algorithms, behind-the-ear EEG, epilepsy, reduced electrode montage, seizure detection, wearable sensors

## 1 | INTRODUCTION

Epilepsy is one of the most common neurological disorders, affecting almost 1% of the population worldwide.<sup>1</sup> Antiepileptic drugs provide adequate treatment for about 70% of patients with epilepsy.<sup>2</sup> The remaining 30% of patients continue to have seizures, drastically reducing their life quality. To obtain efficacy measures of therapeutic interventions for these patients, objective measures of seizure documentation and counting are needed.<sup>3</sup> However, in an outpatient setting, the unreliability of seizure documentation and counting by patients is a major problem.<sup>4–8</sup> Adult patients with focal epilepsy undergoing video-electroencephalographic (EEG) monitoring failed to document around 55% of all recorded seizures and 73% of focal impaired awareness seizures.<sup>6</sup>

Automated seizure detection systems could help to objectively quantify seizures. Those detection systems are typically based on full scalp EEG. In an outpatient setting, full scalp EEG is of limited use because patients will not tolerate wearing a full EEG cap for long time periods during everyday life.<sup>9</sup>

First, research is needed on the recognition of epileptic seizure activity on limited channels, which can be recorded unobtrusively in a nonstigmatizing way. To prove the usefulness of limited channels for seizure detection, an ictal pattern should be visually present on the reduced channel configuration. Previously, the usefulness of single-channel scalp EEG placed behind the earlobe for seizure identification has been investigated.<sup>10</sup> The sensitivity and specificity for recognition of seizures was 86% and 95% for Reviewer 1, 79% and 99% for Reviewer 2. However, only 21 seizures and single-channel derivations were investigated.

Second, algorithms to detect seizures automatically need to be developed using only that limited amount of EEG channels. Previously, reduced electrode montages have been shown useful for seizure detection and documentation for several epilepsy types.<sup>11–14</sup> Our proof-of-concept study showed that behind-the-ear EEG is useful for focal seizure detection.<sup>14</sup> However, the algorithm had false detection rates too high for clinical use.

In this paper, behind-the-ear EEG channels were used that can be recorded with a wearable device.<sup>15</sup> First, a visual analysis was done on 182 seizures by a neurologist to investigate the presence of ictal patterns on the behind-the-ear channels. Second, an algorithm was developed suitable for constructing

**Key Points**

- Recognition of ictal EEG patterns using only behind-the-ear EEG is possible in a significant number of patients with TLE
- A patient-specific seizure detection algorithm using only behind-the-ear EEG resulted in 69.1% sensitivity of 0.49 false detections per day for patients with TLE

a seizure diary offline due to the lower false alarm rate compared to the literature.<sup>14</sup> Two different models were evaluated. The first model was a patient-independent (PI) model, trained with data from different patients. For this PI model, no patient-specific data were needed to train the model, practical in daily life. However, this type of algorithm results in lower performance.<sup>9</sup> The second model was a patient-specific (PS) model, trained with data from the same patient.

This is a class 1 study according to the standards for testing seizure detection devices,<sup>16</sup> because real seizure data from patients with epilepsy were included and gold standard annotations were used for validation. However, the analysis was done retrospectively and the data were not recorded with the dedicated device, but with extra electrodes using traditional scalp EEG.

## 2 | MATERIALS AND METHODS

### 2.1 | Data acquisition

The dataset contained recordings from patients with refractory epilepsy who underwent presurgical evaluation at the University Hospital Leuven (UZ Leuven), Leuven, Belgium. In total, 82 patients were recorded between January 23, 2017 and October 26, 2018. From those patients, 65 were recorded with the extra behind-the-ear electrodes. The developed seizure detection algorithm aims to detect focal seizures with EEG correlates and a length of at least 10 seconds. Therefore, seven patients (11%) without ictal EEG correlates, two patients (3%) with generalized seizures that were too short, and

two patients (3%) with unreadable ictal EEG due to muscle artifacts were excluded from this study. Twelve (18%) patients did not have seizures during the recordings, but were used to evaluate the false detection rate.

The remaining dataset consisted of 54 patients with 5284 hours of data and 182 seizures, recorded in 42 patients. The number of seizures per patient ranged from 1 to 22, with a median of three seizures per patient. The duration of the seizures, the time difference of seizure EEG onset and end, varied between 11 and 695 seconds with a median of 50 seconds. Eighty-nine percent of the seizures were focal impaired awareness seizures. Ninety-one percent of the seizures originated from the (fronto-)temporal lobe. More information about the type, localization, and lateralization can be found in Table 1 and Table S1.

The experimental setup of this study, shown in Figure 1, was the same as for our former publication.<sup>14</sup> The patients were recorded with traditional 10-20 scalp EEG using Ag/AgCl electrodes with a sampling frequency of 250 Hz. Four additional electrodes were glued to the skin behind the ears (two at each side) and were connected to the same EEG amplifier. Using these additional electrodes, four behind-the-ear bipolar channels (two crosshead, one left, and one right bipolar channel) were derived by taking the potential difference between

these electrodes. Figure 2 displays a seizure recorded with the behind-the-ear EEG setup together with the seizure onset.

A clinical expert annotated the seizure onsets and ends with the use of video-EEG data (full channel EEG), validated afterward by a neurologist-epileptologist (W.V.P.). The ethical committee of UZ Leuven approved the study. All patients signed an informed consent form for their participation in this study.

## 2.2 | Visual seizure recognition

Behind-the-ear EEG segments containing seizures and nonseizures were shown to the neurologist-epileptologist (W.V.P.), who was blinded to patient information and recording time. The neurologist was asked to annotate all the segments.

Each 10-minute-long seizure segment contained one seizure with the onset in the middle of the segment. Each 10-minute-long nonseizure EEG segment contained a false detection, obtained with the algorithm described below, in the middle of the segment. The information regarding this onset timing was explained to the neurologist. The duration of 10 minutes was chosen to provide enough preictal and postictal EEG data. The number of nonseizure EEG segments per patient varied randomly between 0.5 and 1.5 times the number of seizure segments. The segments were shown to the neurologist clustered per patient. In total, 182 seizure and 172 nonseizure segments were annotated.

The segments were shown using MATLAB 2017a with EEGLAB graphic interface.<sup>17</sup> The data were shown in a scroll plot using a window of 10 seconds. The plotted data were filtered with a bandpass filter (1-25 Hz), which could be changed. Additionally, the data filtered with a 1-Hz high-pass filter and 50-Hz notch filter were shown. The data were visualized by default between  $-200$  and  $200$   $\mu\text{V}$ , but this scale was adaptable. An example is shown in Figure 2.

To evaluate the performance, sensitivity and specificity were defined as the percentage of recognized and nonrecognized seizure and nonseizure segments, respectively. To summarize the performance measures across the dataset, average values with 95% confidence interval and median with range were calculated.

**TABLE 1** An overview of the seizure types, localization, and lateralization

Seizure type						
	FA	FIA	F-BTC			
n	18	162	2			
Localization						
	Temp	Fronto-temp	Fronto-par	Occipito-temp	Par	NC
n	138	27	2	9	3	3
Lateralization						
	Left	Right	Bilateral	NC		
n	71	94	14	3		

Abbreviations: FA, focal aware; F-BTC, focal to bilateral tonic-clonic; FIA, focal impaired awareness; n, number of seizures; NC, not clear; par, Parietal; temp = Temporal.

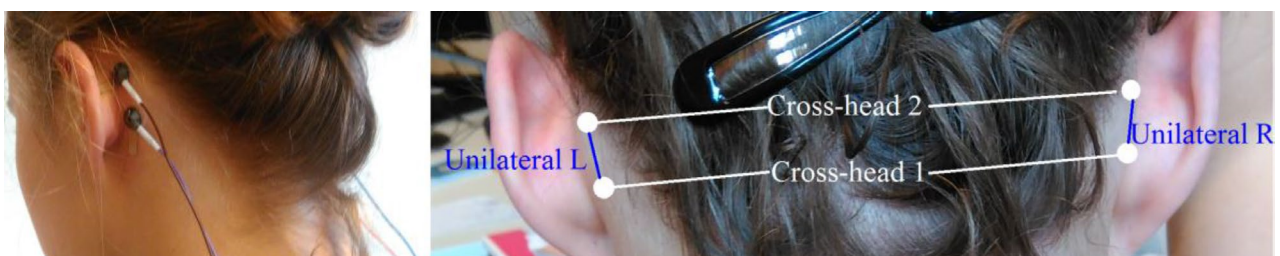


**FIGURE 1** Behind-the-ear electroencephalographic setup. Left panel shows extra behind-the-ear electrodes glued to the skin. Right panel shows bipolar channel derivations. Reproduced with permission from Gu et al<sup>14</sup>

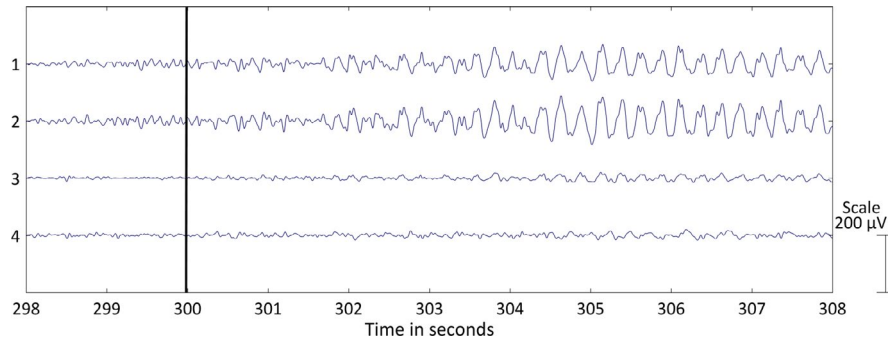


**FIGURE 2** Left temporal lobe seizure recorded with behind-the-ear electroencephalographic (EEG) setup. The four bipolar EEG channels are shown over a period of 10 seconds: (1) crosshead 1, (2) crosshead 2, (3) unilateral left, (4) unilateral right. The bipolar EEG channels were filtered with a bandpass filter (1-25 Hz). The black horizontal line at 300 seconds depicts the seizure onset

## 2.3 | Automated seizure detection

The automated seizure detection algorithm was applied twice with two different aims. The aim of algorithm I was to detect all annotated seizures with ictal EEG correlate using video-EEG (full EEG). All those seizures were included in the training and test set. The aim of algorithm II was to detect only those seizures that were recognized on the behind-the-ear EEG by the neurologist. Here, only those recognized seizures were included in the training and test set. The PI model was applied on all patients. However, the PS model could only be applied on patients with at least two seizures, because one seizure was needed to train the model and one seizure to test the model.

The different steps of the algorithm are explained: preprocessing, feature extraction, feature normalization, classification, cross-validation, and postprocessing with the algorithm evaluation criteria.

### 2.3.1 | Preprocessing

As input, three bipolar behind-the-ear EEG channels were used: crosshead channel 2, and the unilateral left and right channels. Each bipolar channel was filtered with a bandpass filter (1-25 Hz). After filtering, the data were segmented in 2-second windows with 50% overlap. Windows with a root mean square amplitude greater than  $150 \mu\text{V}$  or less than  $13 \mu\text{V}$  were removed from the analysis, because those windows contained high-amplitude artifacts or contained only background EEG.

### 2.3.2 | Feature extraction

Features, taken from literature, were extracted from each channel and each window, unless removed by the preprocessing. Time domain and frequency domain features were extracted.<sup>18</sup> Two extra frequency domain features were extracted, mean and normalized power in the high-frequency band between 40 and 80 Hz (before applying the bandpass

**TABLE 2** Extracted features

Time domain	1-3. Number of zero crossings, maxima, and minima <sup>17</sup> 4. Skewness <sup>17</sup> 5. Kurtosis <sup>17</sup> 6. Root mean square amplitude <sup>17</sup>
Frequency domain	7. Total power <sup>17</sup> 8. Peak frequency <sup>17</sup> 9-16. Mean (9-12) and normalized (13-16) power in frequency bands: delta (1-3 Hz), theta (4-8 Hz), alpha (9-13 Hz), beta (14-20 Hz) <sup>17</sup> 17-18. Mean (17) and normalized (18) power in HF band (40-80 Hz)
Entropy derived	19. Sample entropy <sup>19</sup> 20. Shannon entropy <sup>18</sup> 21. Spectral entropy <sup>18</sup>
Asymmetry	22-25. Power asymmetry in frequency bands: delta (1-3 Hz), theta (4-8 Hz), alpha (9-13 Hz), beta (14-20 Hz) <sup>20</sup>

Abbreviation: HF, high-frequency.

filter) to discriminate between artifacts and seizure activity. Entropy-based features were also added.<sup>19,20</sup> Finally, the power asymmetry at different frequency bands was calculated.<sup>21</sup> Here, the power asymmetry was calculated between the left and right channel. A list of all the features can be found in Table 2. Features 1-21 were calculated for all three channels, whereas features 22-25 resulted in one feature for each frequency band. This resulted in a total of 67 features.

### 2.3.3 | Feature normalization

Because differences in the EEG amplitude were present between individuals, and amplitude variations occurred over time, normalization was crucial. The median decaying

memory method was shown to be the best approach using line length features.<sup>22</sup> This normalization method was applied on all the amplitude-dependent features, which were the root mean square amplitude, total power, and mean power in the different frequency bands (features 6, 7, 9-12, and 17 in Table 2). Additionally, log transformation was applied on features 5-7, 9-12, 14, 15, 17, 18, and 20, selected visually by comparing the distribution before and after log transformation. Features 1-21 were calculated for all three channels. For each feature, the left and right channel values were sorted largest to smallest,<sup>23</sup> which removed information about the spatial seizure location. This step is important because both left and right seizures were present in the training and test sets.

### 2.3.4 | Classification

To classify each 2-second window, support vector machine (SVM) with a radial basis function kernel was used. To account for the class imbalance from the dataset (ie, very few training examples in the seizure vs the nonseizure class), Weighted SVM<sup>24,25</sup> was applied. To find the optimal classifier, the SVM minimizes the misclassification of training data points. To account for class imbalance, the cost given to each nonseizure data point is  $N^+ + N^- / 2 * N^+$ , whereas the cost given to each seizure data point is  $N^+ + N^- / 2 * N^-$  with  $N^+$  and  $N^-$  representing the number of data points belonging to the nonseizure and seizure class, respectively. The values of the hyperparameters were selected using a fivefold cross-validation using the training set for the PI model. The most frequently selected values for those parameters were used for the PS model, because not enough data were available to perform a cross-validation on the training set.

Nonseizure training data were selected from the first 24-hour EEG recording, as this period covers the different brain states.<sup>26</sup> To cover as many different EEG patterns as possible from the nonseizure vigilance states, 1-minute long segments, consisting of 30 nonoverlapping 2-second windows, recorded every 15 minutes, were selected.<sup>17</sup> From this selection, 100 and 150 nonseizure windows were randomly sampled per patient for training the PI and PS classifiers.

Seizure training segments of 10 seconds,<sup>14,18</sup> further split into 2-second windows, during each seizure were selected visually at the seizure onset by the first author. A length of 10 seconds was chosen to give each seizure, short or long, the same importance in the classifier, as the minimum seizure duration was 10 seconds. Visual selection by the first author was needed to include a typical ictal pattern in the training set and to avoid attenuation at the start of the seizure or artifacts.

### 2.3.5 | Cross-validation

Only a single retrospective dataset was available for the study. However, different nonoverlapping folds of the dataset were used for training and testing purposes. The cross-validation for the PI model was leave-one-patient-out. The cross-validation for the PS model was leave-one-seizure-out. The fold splits were set exactly in the middle of the nonseizure data between two seizures. The test set, the fold left out for training, was a continuous tract that contained all the nonseizure/seizure data in that fold, that is, various vigilance states and the direct neighborhood of a seizure.

### 2.3.6 | Postprocessing

To generate a seizure detection, eight of 10 consecutive 2-second overlapping windows should be classified as seizure by the model. Ten consecutive windows were chosen, because the minimal duration of a seizure was taken as 10 seconds. To allow for small artifacts during a seizure, only eight of the windows should be classified as seizure.

### 2.3.7 | Algorithm evaluation

The following measures were applied to determine the performance of the seizure detection algorithm:

1. Detection sensitivity:  $TP / (TP + FN)$ , where TP = true positive and FN = false negative. A seizure was detected correctly (TP) if the detection occurred between the EEG onset and end of the seizure.
2. False positive (FP) detection rate per 24 hours: FPs/recording length; FPs within 10 seconds of each other were counted as one FP.
3. Detection delay: the time interval between the EEG seizure onset and detection by the algorithm.
4. Positive predictive value (PPV):  $TP / (TP + FP)$ .
5. F1-score:  $2 * (PPV * Recall) / (PPV + Recall)$  with Recall =  $TP / (TP + FN)$ .

To summarize the performance measures across the dataset, the averages including their 95% confidence intervals and medians with their range were calculated.

## 3 | RESULTS

### 3.1 | Visual seizure detection

The neurologist identified 114 of 182 seizure segments and 161 of 172 nonseizure segments in total. An average

sensitivity of 65.7% and specificity of 94.4% was obtained, as shown in Table 3. In Table S2, the results per patient are shown.

Figure 3 shows the sensitivities for the different seizure types (A), localization (B), lateralization (C), and seizure duration (D). The sensitivities were calculated as percentage recognized seizures in that category over the whole database. Sensitivity for focal impaired awareness seizures was 59%, for focal aware (FA) seizures 89%, and for focal to bilateral tonic-clonic seizures 100%. The temporal, frontotemporal, and occipitotemporal lobe seizures had a sensitivity of 62%, 85%, and 22%, respectively. The frontoparietal and parietal seizures had 0% and 67% sensitivity. The bilateral group had lower sensitivities (43%) than the lateralized groups, left 58% and right 70%, respectively. The sensitivity increased with the seizure duration.

### 3.2 | Automated seizure detection

An overview of the results of the PI and PS model with the two different aims, detecting all the seizures and detecting the seizures recognized on behind-the-ear EEG, are shown in Table 3. In Table S2, the results per patient are shown. The PI model resulted in an average sensitivity of 72.7% (aim I) and 64.1% (aim II), whereas the FP rate decreased from 34.2 FPs/24 hours (aim I) to 2.8 FPs/24 hours (aim II). The PS model resulted in a higher average sensitivity of 69.1% (aim II) compared to 63.4% (aim I), whereas the FPs/24 hours rate was 0.88 (aim I) and 0.49 (aim II). By analyzing the 24 patients tested with the PS model (aim II), the number of patients with a sensitivity  $\geq 60\%$  and FPs/24 hours  $\leq 1$  was nine with the PI model and 15 with the PS model.

The PI model with aim II detected 14 extra seizures, from six patients, which the neurologist did not recognize. The PS model with aim II detected 4 extra seizures, from four patients, which were not annotated on the full scalp EEG, but recognized with hindsight. Note that these seizures were not taken into account for calculating the sensitivity of aim II.

## 4 | DISCUSSION

### 4.1 | Visual seizure recognition

Average sensitivity for visual recognition of seizures on behind-the-ear EEG was 65.7% (ie, 68 of 182 seizures were not recognized), which was lower than expected, because the database mostly consisted of temporal lobe seizures and the behind-the-ear electrodes were closely located to the temporal lobe. To explain these results, the neurologist inspected the behind-the-ear EEG again, together with the full EEG, and identified three main reasons for missed

seizures in the behind-the-ear EEG. Most importantly, 63 seizures (93%) that were not recognized on behind-the-ear EEG contained artifacts, mainly muscle. In 11 seizures, a salt bridge was present in a channel that was crucial for seizure recognition. This salt bridge, which is the smearing of electrode paste between electrodes causing a very low impedance ( $\sim$ short circuit), was recognized due to a lower frequency and amplitude content of one bipolar channel compared to the background.<sup>27</sup> Full scalp EEG of the same seizures contained the same artifacts at the location of the behind-the-ear electrodes, but the ictal patterns were visible in other channels. Second, 39 seizures (57%) had only subtle ictal EEG patterns on the full EEG. Those seizures were annotated taking the presence of a clinical seizure on video into account. This information was not available when reviewing behind-the-ear EEG blindly. Third, 29 seizures (43%) had a bilateral ictal pattern from the onset, which was more difficult to pick up with the crosshead channels, where the ictal discharges were less obvious due to differential amplification of the relatively symmetric signals. Typical lateralized recruiting theta patterns, as in Figure 1, were easily recognized. We conclude that a majority of temporal lobe seizures are recognized on behind-the-ear EEG, but the impact of artifacts in the recognition of seizures is higher when only a limited number of electrodes and channels are available as compared with a full EEG.

The neurologist annotated 11 of the 172 nonseizure segments as a seizure. With hindsight, four segments did contain a seizure on the full EEG and were actually correctly annotated on the behind-the-ear EEG. Those seizures were missed during the first annotation session of the video-EEG. Four segments contained artifacts, which the neurologist annotated as a seizure, which could have been avoided by looking at the unfiltered EEG. One segment did not seem to contain an ictal pattern on second examination. Two segments contained the appearance of an occipital alpha rhythm, which was clear on the full EEG, but was interpreted as an ictal pattern on the behind-the-ear EEG. We conclude that with a conservative reading of behind-the-ear EEG, specificity is very high (around 96%).

The higher sensitivity for visual recognition on behind-the-ear EEG of FA seizures (89%) compared to the focal impaired awareness seizures (59%) was not expected, because only 15%-30% of FA seizures contain ictal EEG changes.<sup>28</sup> However, we included in this study only seizures with an ictal EEG correlate. Furthermore, the dataset contained 28 FA seizures in four different patients, who had respectively one (not detected), 14 (all detected), two (all detected), and one (not detected) seizures. By averaging the sensitivity across patients, an average sensitivity of 50% was obtained. A higher sensitivity for the temporal lobe group compared to the extratemporal lobe group was expected, because behind-the-ear electrodes are closer to the temporal lobe. However, it is interesting that we could pick up two of three parietal lobe seizures, which

**TABLE 3** Results of visual seizure recognition (Sens and Spec) and automated seizure detection I with aim of detecting all seizures annotated on video-EEG and automated seizure detection II with aim of detecting only seizures recognized by the neurologist on behind-the-ear EEG for PS and PI models (number of patients and seizures, Sens, false detection rate, PPV, detection delay, and F1-score)

A. Average [95% confidence interval]						
Visual seizure recognition						
	Patients, n (seizures, n)	Sens, %	Spec, %			
	42 (182)	65.7 [54-77]	94 [89-99.9]			
Automated seizure detection I						
	Patients, n (seizures, n)	Sens, %	FPS/24 h	PPV, %	Delay, s	F1-score
PI	54 (182)	72.7 [61-84]	34.2 [17-51]	11.5 [6-17]	22.4 [17-28]	0.16 [0.09-0.23]
PS	36 (176)	63.4 [51-76]	0.88 [0.4-1.4]	57.3 [43-71]	21.6 [18-26]	0.57 [0.45-0.70]
Automated seizure detection II						
	Patients, n (seizures, n)	Sens (%)	FPS/24 h	PPV, %	Delay, s	F1-score
PI	54 (114)	64.1 [50-79]	2.8 [1.3-4.3]	38.9 [25-52]	22.8 [18-28]	0.38 [0.26-0.50]
PS	24 (103)	69.1 [54-84]	0.49 [0.1-0.9]	65.4 [49-81]	20.2 [15-26]	0.62 [0.46-0.78]
B. Median [range]						
Visual seizure recognition						
	Patients, n (seizures, n)	Sens, %	Spec, %			
	42 (182)	70.8 [0-100]	100 [0-100]			
Automated seizure detection I						
	Patients, n (seizures, n)	Sens, %	FPS/24 h	PPV, %	Delay, s	F1-score
PI	54 (182)	100 [0-100]	13.6 [0-384]	3.4 [0-100]	17 [3-77]	0.07 [0-1]
PS	36 (176)	67.4 [0-100]	0 [0- 4.2]	63 [0-100]	18 [10-56]	0.64 [0-1]
Automated seizure detection II						
	Patients, n (seizures, n)	Sens, %	FPS/24 h	PPV, %	Delay, s	F1-score
PI	54 (114)	100 [0-100]	1.2 [0-31.5]	23 [0-100]	20 [3-56]	0.29 [0-1]
PS	24 (103)	83.3 [0-100]	0 [0-3.7]	72 [0-100]	16 [9-65]	0.72 [0-1]

Abbreviations: EEG, electroencephalography; FP, false positive; PI, patient-independent model; PPV, positive predictive value; PS, patient-specific model; Sens, sensitivity; Spec, specificity.

indicates that ictal discharges arising from extratemporal lobes propagate to the behind-the-ear electrodes. However, further testing needs to be done on seizures originating from other lobes to determine whether the seizures are visible on the behind-the-ear channels. The bilateral group (43%) had lower sensitivity than the left (58%) and right (70%) groups, because a bilateral ictal pattern was more difficult to pick up with the crosshead channels due to differential amplification of the relatively symmetric signals. The increased sensitivity with seizure length was expected, because longer seizures are often associated with stronger ictal discharges.

## 4.2 | Automated seizure detection

The PI seizure detection algorithm had lower performance compared to the PS algorithm for both aims I and II; in particular, the FP rate of the PS algorithm was decreased and PPV was increased. This is in agreement with the literature, as ictal behavior is highly patient-specific.<sup>9</sup>

The algorithm with aim II improved the results compared to aim I, because subtle ictal EEG patterns and seizures with artifacts, which were not recognized by the neurologist, were left out from the test set. Furthermore, leaving out these unclear and artifacted seizures also resulted in a better training set, which in turn led to a better classifier and a lower FP rate for aim II.

The PS algorithm aim II had in total 22 false detections. The reasons for those false detections were diverse: high-amplitude artifacts in two channels, probably due to a technical problem with one EEG behind-the-ear electrode ( $n = 1$ ); slightly higher amplitude and change in frequency power, which are characteristics of ictal EEG ( $n = 2$ ); seizures that were missed while annotating the video-EEG ( $n = 4$ ); chewing artifacts ( $n = 9$ ); high-frequency artifacts, probably due to muscle activity ( $n = 5$ ); and a technical artifact (flat line;  $n = 1$ ). The reasons for the FPS of the PI algorithm aim II were similar, most frequently high-frequency artifacts.

Large differences were observed between the mean and average results, because outliers were present. Outliers for

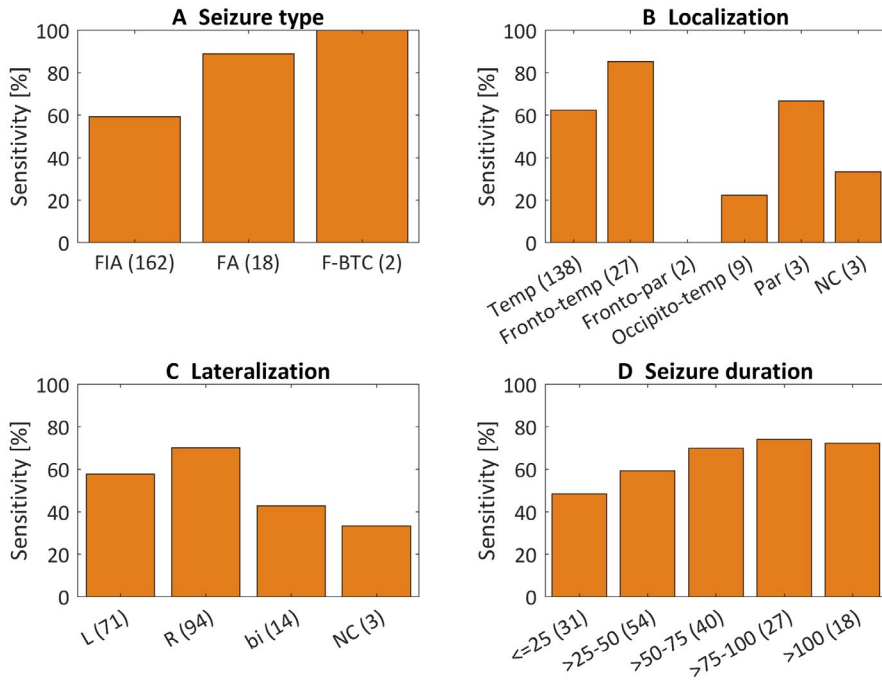


**FIGURE 3** Sensitivities for the different seizure types (A), localizations (B), lateralizations (C) and seizure durations in seconds (D) are plotted for the patient-independent model with aim I and visual recognition study. The sensitivities were calculated as percentage recognized seizures in that category over whole the database. bi, bilateral; FA, focal aware; F-BTC, focal to bilateral tonic-clonic; FIA, focal impaired awareness; L, left; NC, not clear; par, parietal; R, right; temp, temporal

the PS algorithm (three patients had a sensitivity of 0%) were often due to the limited amount of training data, which caused overfitting of the model. This resulted in low sensitivity if the test seizures were different from the training seizures. Outliers for the PI algorithm, especially for aim I (two patients had a false alarm rate higher than six per hour), were caused by a combination of three main reasons: large power in the theta band, high-frequency artifacts, and a salt bridge in the right channel. This caused a lateralization, which is typical for unilateral seizures.

In this study, the EEG was measured behind the ears, as shown in Figure 1. However, recently it has been shown that EEG recorded with a small device in the ear can detect temporal lobe seizures<sup>29</sup> and generalized tonic-clonic seizures.<sup>30</sup> A similar visual seizure recognition study for temporal lobe seizures resulted in comparable performances.<sup>29</sup> Those results suggest that the signals of both behind-the-ear and in-the-ear EEG could be used to detect temporal lobe seizures. However, the design of the devices is different. An advantage of the in-the-ear EEG is the discreteness, but disadvantages are the possible hearing loss, discomfort, and need for individualized design.

### 4.3 | Clinical use of algorithm

A PI algorithm is more suitable for clinical use, because one device with the same algorithm can be given to all patients and no ictal EEG data are required beforehand. In this study, 24 patients had a sensitivity > 50% with the PI algorithm, tested on 35 patients. Originally, 65 patients were recorded with the behind-the-ear electrodes, so 37% of the patients in this study

could potentially benefit from a device with a PI algorithm. One hundred eighty-two seizures were recorded, 114 (63%) were identified by the doctor and 71 (39%) were detected with the algorithm. Those values might seem to be low, but they were better than self-reporting by patients. Only 27% of focal impaired awareness seizures were reported by patients.<sup>6</sup> However, the false detection rate of the PI algorithm was high (2.8 FPs/24 hours) and PPV was low (38.9%). Those could be improved by personalizing the algorithm. The PS algorithm had lower FPs/24 hours (0.49) and higher PPV (65.4%).

Although PS algorithms are in general impractical, they can be useful in certain scenarios. They could be used in patients with refractory temporal lobe epilepsy who have video-EEG recordings of their habitual seizures. Using this patient-specific ictal EEG data, the algorithm could be trained automatically with minimal time investment by the clinician. The neurologist only needs to provide the annotations for the start and end of the seizures, which is usually part of the clinical review of video-EEG recordings.

### 4.4 | Future work

The ictal EEG data used in this study were recorded with the hospital system using Ag/AgCl electrodes. The recorded patients were hospitalized, which limits the movements and artifacts present in the data. We showed that artifacts may have an important impact in the correct interpretation of seizures recorded with behind-the-ear EEGs. The algorithm should be tested on behind-the-ear EEG data, recorded with a wearable device<sup>15</sup> in an outpatient setting as written in the standards for testing and clinical validation.<sup>16</sup> The preprocessing, more

specifically the removal of artifacts, should be adapted to the wearable data.

Training and testing the algorithm was done using the same database, and a retrospective analysis was performed. To extend the research, separate databases need to be used for training and testing and prospective analysis needs to be performed.<sup>16</sup>

In this work, SVMs were used as classifiers. Other classifiers, for example, random forest,<sup>31</sup> should be implemented and tested.

Behind-the-ear EEG is not the only type of signal suitable for a wearable seizure detection system in an outpatient setting. Electrocardiography (ECG), which can be recorded in an outpatient setting, has added value to automatically detect seizures in temporal lobe epilepsy patients.<sup>25,32–35</sup> Previous studies investigated multimodal seizure detection algorithms.<sup>11</sup> A multimodal algorithm should be developed combining information from behind-the-ear EEG and ECG, recorded with wearable devices in an outpatient setting. We are currently validating our wearable device measuring behind-the-ear EEG, movement, and ECG in a multicenter study<sup>36</sup> (EIT Health: SeizeIT<sup>2</sup><sup>37</sup>).

## ACKNOWLEDGMENTS

This study was supported by Bijzonder Onderzoeksfonds (BOF) KU Leuven: "Prevalence of Epilepsy and Sleep Disturbances in Alzheimer Disease" (C24/18/097); EIT Health: 19263 SeizeIT2, "Discreet Personalized Epileptic Seizure Detection Device"; and the Flanders AI Research Program.

## CONFLICT OF INTEREST

None of the authors has any conflict of interest to disclose. We confirm that we have read the Journal's position on issues involved in ethical publication and affirm that this report is consistent with those guidelines.

## ORCID

Kaat Vandecasteele  <https://orcid.org/0000-0002-9888-577X>

Wim Van Paesschen  <https://orcid.org/0000-0002-8535-1699>

## REFERENCES

- Forsgren L, Beghi E, Oun A, Sillanpää M. The epidemiology of epilepsy in Europe—a systematic review. *Eur J Neurol*. 2005;12:245–53.
- French JA. Refractory epilepsy: clinical overview. *Epilepsia*. 2007;48:3–7.
- Elger CE, Mormann F. Seizure prediction and documentation—two important problems. *Lancet Neurol*. 2013;12:531–2.
- Blum DE, Eskola J, Bortz JJ, Fisher RS. Patient awareness of seizures. *Neurology*. 1996;47:260–4.
- Fisher RS, Blum DE, DiVentura B, et al. Seizure diaries for clinical research and practice: limitations and future prospects. *Epilepsy Behav*. 2012;24:304–10.
- Hoppe C, Poepel A, Elger CE. Epilepsy: accuracy of patient seizure counts. *Arch Neurol*. 2007;64:1595–9.
- Poohikian-Sarkissian S, Tai P, del Campo M, et al. Patient awareness of seizures as documented in the epilepsy monitoring unit. *Can J Neurosci Nurs*. 2009;31:22–3.
- Tatum WO, Winters L, Gieron M, et al. Outpatient seizure identification: results of 502 patients using computer-assisted ambulatory EEG. *J Clin Neurophysiol*. 2001;18:14–9.
- Baumgartner C, Koren JP. Seizure detection using scalp-EEG. *Epilepsia*. 2018;59:14–22.
- Bennis FC, Geertsema EE, Velis DN, Reus EE, Visser GH. The use of single bipolar scalp derivation for the detection of ictal events during long-term EEG monitoring. *Epileptic Disord*. 2017;19:307–14.
- Fürbass F, Kampusch S, Kaniusas E, et al. Automatic multimodal detection for long-term seizure documentation in epilepsy. *Clin Neurophysiol*. 2017;128:1466–72.
- Sopic D, Aminifar A, Atienza D. e-glass: a wearable system for real-time detection of epileptic seizures. Paper presented at: IEEE International Symposium on Circuits and Systems (ISCAS). May 2018.
- Kjaer TW, Sorensen HBD, Groenborg S, Pedersen CR, Duun-Henriksen J. Detection of paroxysms in long-term, single-channel EEG-monitoring of patients with typical absence seizures. *IEEE J Transl Eng Health Med*. 2017;5:1–8.
- Gu Y, Cleeren E, Dan J, et al. Comparison between scalp EEG and behind-the-ear EEG for development of a wearable seizure detection system for patients with focal epilepsy. *Sensors*. 2017;18:1–19.
- Boeckx S, Van Paesschen W, Bonte B, Dan J. Live demonstration: SeizeIT—a wearable multimodal epileptic seizure detection device. Presented at: 2018 IEEE Biomedical Circuits and Systems Conference (BioCAS); October 17–19, 2018; Cleveland, OH.
- Beniczky S, Ryvlin P. Standards for testing and clinical validation of seizure detection devices. *Epilepsia*. 2018;59:9–13.
- Delorme A, Makeig S. EEGLAB: an open source toolbox for analysis of single-trial EEG dynamics including independent component analysis. *J Neurosci Methods*. 2004;134:9–21.
- Hunyadi B, Signoretto M, Van Paesschen W, Suykens JA, Van Huffel S, De Vos M. Incorporating structural information from the multichannel EEG improves patient-specific seizure detection. *Clin Neurophysiol*. 2012;123:2352–61.
- Greene BR, Faul S, Marnane WP, Lightbody G, Korotchikova I, Boylan GB. A comparison of quantitative EEG features for neonatal seizure detection. *Clin Neurophysiol*. 2008;119:1248–61.
- Song Y, Liò P. A new approach for epileptic seizure detection: sample entropy based feature extraction and extreme learning machine. *J Biomed Sci Eng*. 2010;3:556.
- Hunyadi B, De Vos M, Van Paesschen W, Van Huffel S. A mimicking approach for human epileptic seizure detection. Paper presented at: Biosignal 2010: International Biosignal Processing Conference; July 14–16, 2010; Berlin, Germany.
- Logesparan L, Rodriguez-Villegas E, Casson AJ. The impact of signal normalization on seizure detection using line length features. *Med Biol Eng Comput*. 2015;53:929–42.
- Greene BR, Boylan GB, Reilly RB, de Chazal P, Connolly S. Combination of EEG and ECG for improved automatic neonatal seizure detection. *Clin Neurophysiol*. 2007;118:1348–59.

24. Akbani R, Kwek S, Japkowicz N. Applying support vector machines to imbalanced datasets. In: Boulicaut JF, Esposito F, Giannotti F, Pedreschi D, eds. *Machine Learning: ECML 2004*. Berlin, Heidelberg, Germany: Springer; 2004:39–50.
25. De Cooman T, Varon C, Hunyadi B, Van Paesschen W, Lagae L, Van Huffel S. Online automated seizure detection in temporal lobe epilepsy patients using single-lead ECG. *Int J Neural Syst*. 2017;27:1750022.
26. Qu H, Gotman J. A patient-specific algorithm for the detection of seizure onset in long-term EEG monitoring: possible use as a warning device. *IEEE Trans Biomed Eng*. 1997;44:115–22.
27. Stern JM. *Atlas of EEG Patterns*. Philadelphia, PA: Lippincott Williams & Wilkins; 2005.
28. Devinsky O, Kelley K, Porter RJ, Theodore WH. Clinical and electroencephalographic features of simple partial seizures. *Neurology*. 1988;38:1347–52.
29. Zibrandtsen IC, Kidmose P, Christensen CB, Kjaer TW. Ear-EEG detects ictal and interictal abnormalities in focal and generalized epilepsy—a comparison with scalp EEG monitoring. *Clin Neurophysiol*. 2017;128:2454–61.
30. Zibrandtsen IC, Kidmose P, Kjaer TW. Detection of generalized tonic-clonic seizures from ear-EEG based on EMG analysis. *Seizure*. 2018;59:54–9.
31. Manzouri F, Heller S, Dümpelmann M, Woias P, Schulze-Bonhage A. A comparison of machine learning classifiers for energy-efficient implementation of seizure detection. *Front Syst Neurosci*. 2018;12:43.
32. Leutmezer F, Scherthaner C, Lurger S, Pötzelberger K, Baumgartner C. Electrocardiographic changes at the onset of epileptic seizures. *Epilepsia*. 2003;44:348–54.
33. Eggleston KS, Olin BD, Fisher RS. Ictal tachycardia: the head-heart connection. *Seizure*. 2014;23:496–505.
34. Jeppesen J, Beniczky S, Johansen P, Sidenius P, Fuglsang-Frederiksen A. Using Lorenz plot and Cardiac Sympathetic Index of heart rate variability for detecting seizures for patients with epilepsy. *Conf Proc IEEE Eng Med Biol Soc*. 2014;2014:4563–6.
35. Vandecasteele K, De Cooman T, Gu Y, et al. Automated epileptic seizure detection based on wearable ECG and PPG in a hospital environment. *Sensors*. 2017;17:2338.
36. Van Paesschen W. The future of seizure detection. *Lancet Neurol*. 2018;17:200–2.
37. EIT Health. SeizeIT2. 2018. Available at: <https://www.eithealth.eu/seizeit2>. Accessed September 29, 2019.

## SUPPORTING INFORMATION

Additional supporting information may be found online in the Supporting Information section.

**How to cite this article:** Vandecasteele K, De Cooman T, Dan J, et al. Visual seizure annotation and automated seizure detection using behind-the-ear electroencephalographic channels. *Epilepsia*. 2020;00:1–10. <https://doi.org/10.1111/epi.16470>